

Development of a reconstruction code for neutron tomography

Jin Man Kim^a, TaeJoo Kim^{a*}, Jongyul Kim^a

^aNeutron Science Center, Korea Atomic Energy Research Institute, Daejeon, 34057, Republic of Korea

*Corresponding author: tj@kaeri.re.kr

1. Introduction

A neutron radiography is widely used in various research and industry sectors, which is complementary to x-ray due to the different characteristics [1–3]. In particular, the neutron radiography is used to obtain information for inner structures of some materials such as metals because it can penetrate metals.

In addition, when multiple images captured while the object rotates at an angle of a particular unit are reconstructed, the three-dimensional view can be made that is a neutron tomography. It means that we can identify the cross-section of the object. Therefore, a neutron tomography is an essential technology that can be used in the cultural investigation, defense, aviation and various other industries because it allows accurate observation of the interior without damaging objects.

To see a cross-section of an object using images taken while rotating, complex image processing is required, and usually, a commercial program is used. However, commercial programs would be costly to maintain. Also, if additional analysis using features not supported by the program is required, additional costs will be incurred. Even if users find another program to make an additional analysis, it is very inefficient in terms of time and cost if users analyze it using various programs every time.

In this regard, developing a reconstruction code can save on maintenance costs in the future. Besides, it can save money and time in the long term because the features that are needed can be freely added. Users can freely apply and add more advanced theories so that the developed code can be expanded easily and can yield better results.

2. Background

In order to reconstruct the 2D images taken from the side of the object, a large amount of image operation is required. Radon transform is one of the most important things during image processing. Radon Transform is a representation of projection images for tomographic scan according to the change of angle. It can be obtained by rearranging the 2D images obtained by rotating the object.

Fig. 1 is a schematic image of how to obtain a sinogram. An object with a constant height is captured from four directions using neutron radiography as shown in Fig. 1(a). After taking images, a sinogram can be obtained by combining lines of the images of all angles with respect to a specific z value into a single

array as like Fig. 1(c). This image is called a sinogram. If a sinogram is made at 1-degree intervals instead of 4 directions (90 degrees), a smoother waveform image is observed as shown in Fig. 1(d).

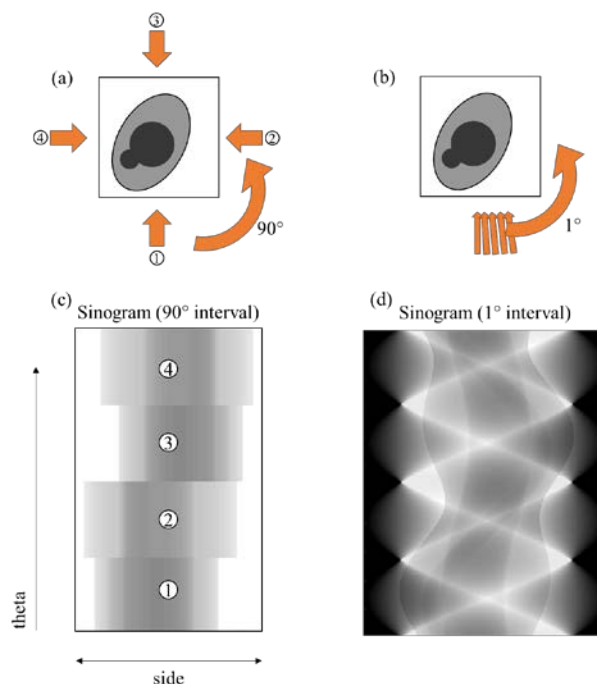


Fig.1 Difference of the sinograms depending on the rotation interval.

A cross-section image can be obtained by performing an inverse Radon transform on the sinogram. Fig. 2 shows the sinograms and reconstructed images with varying rotation intervals. The smaller the interval of the rotation angle is, the more accurately the original shape is obtained. Therefore, if the rotation angle is small enough when the neutron images are captured, the reconstructed image will show the internal structure of the object very accurately.

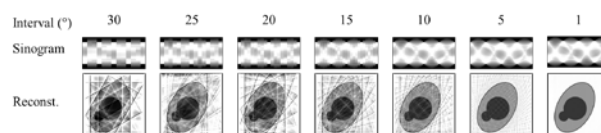


Fig. 2 Difference of the reconstructed images depending on the rotation interval.

3. Process & result

3.1 Experimental setup

The image data used for the development of the code were taken using the Neutron Radiography Facility

(NRF) of HANARO in Korea Atomic Energy Research Institute. The sample was a preliminary experimental test set containing a model of hidden relics, Korean paper, and rice in a copper box. A small Buddha statue was placed inside a large Buddha statue. All the stuffs were put inside the copper box. Then, the objects inside the copper box were observed using a neutron radiography. Matlab (2018a) with an image processing toolbox was used for the development of the code.



Fig. 3 Set of hidden relic samples with copper box.

3.2 Image correction

If the image is taken using neutron radiography, it will include white spots. This does not occur if the shielding is ideal, but there is a limitation to the shielding due to the spatial and expense problem, which causes the CCD sensor to be exposed to gamma. Perfect shielding requires very high cost, time, and space, but it is very difficult to realistically accomplish the perfect shielding, so we supplemented it with image processing.

The algorithm to remove the white spot is as shown in Fig. 4. We effectively removed only the white spot by replacing the white spot after making the mask using the Median filter. In the present study, the filter level was set to 4×4, and the threshold was arbitrarily selected according to the image to remove the white spot.

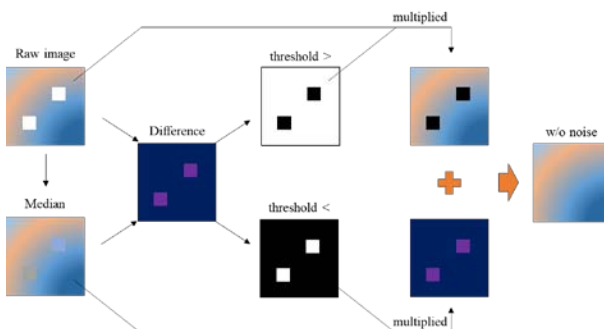


Fig. 4 The method of the noise reduction.

In addition, gradients appeared in brightness due to non-uniform beam intensity depending on the position when images were captured. Therefore, normalization was performed by using the open beam image taken when there was no sample and the dark image taken when there was no beam. The normalization was performed by the following equation. In this study, 15 images were taken for white and dark images, respectively.

$$I_{normalized} = \frac{I_{sample} - I_{dark}}{I_{white} - I_{dark}}$$

3.3 Correction of a rotation axis

When taking tomographic scans, a rotation axis may be inclined due to the misaligned sample stage, the horizontal and the position of the camera, or it may deviate from the center of the screen. Therefore, through the image analysis, it is necessary to compensate for the angle of the rotation axis and to move the axis at the center of the image plane. Otherwise, distorted images are acquired after reconstruction.

Two image sets were used for the axis correction as shown in Fig. 5(a). Since the second image was taken when the object was rotated 180°, it overlapped with the first image when the second image was flipped. Using this relationship we found the rotation axis. When the profile was obtained for one z-value in the first image (y-value in the image plane), the value changed abruptly at the boundary of the object as shown in Fig. 5(b). Raw data profiles were smoothed to ignore meaningless fluctuations because of the noise.

The smoothing process was repeated 100 times in order to obtain a sufficiently smooth curve after redefining the value by averaging five data around each pixel. Then the maximum or minimum point of the effective rate of change was detected as shown in Fig. 5(c).

In Fig. 5 (c), the position where the rate of change rapidly decreased in the first image became a position where the rate of change rapidly increased in the second image. The center point could be obtained by finding the average of these positions. By repeating this process with few z-values, we found the tilt of the rotation axis and saw how far the center was off the center of the image plane. In this study, five z-values were used for the correction of the rotation axis.

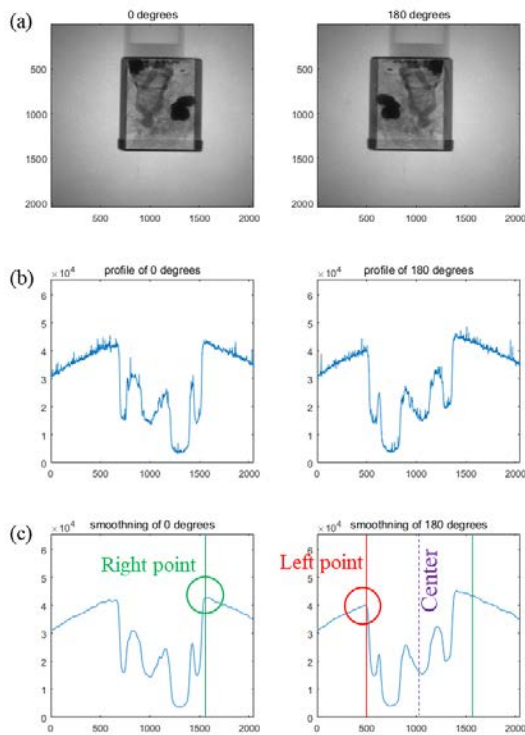


Fig. 5 Profile analysis for the detection of the rotation axis.

Normalized images were used for the axis correction, and the rotation axis was slightly inclined as shown in Fig. 6. In addition, the sample table (the shape of a rectangular shell at the bottom of the object) used for rotation deviated from the center of the image plane. Using the algorithm described above, the rotation axis was aligned vertically and the rotation axis was moved to the center of the image.

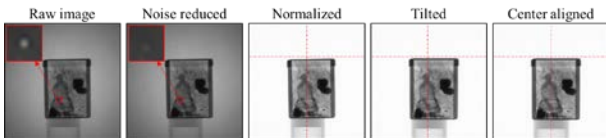


Fig. 6. Image preparation for the reconstruction.

3.3 Sinograms

After the rotation axis correction, sinograms were generated by stacking pixel values of all angles with respect to each z-value. Only the pixel values of images taken at all angles for one slice were extracted and rearranged. Then, the sinogram was expressed along the z-axis as shown in Fig. 7.

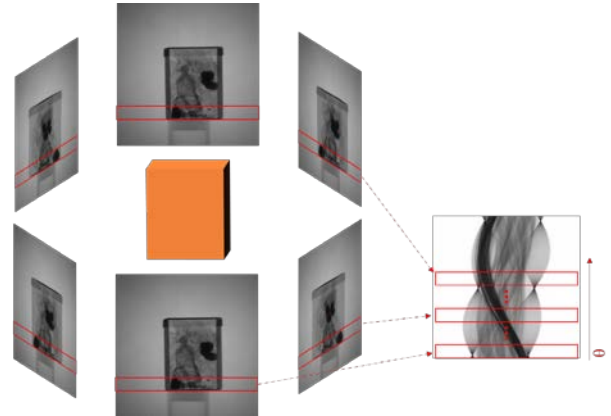


Fig. 7 Stacking images for a sinogram.

As a result, the wave pattern was very clear. The smoothness of these waveshapes without interruption means that the sinogram was well formed. As shown in Fig. 8, the wave shape and intensity varied depending on the position of the slice.

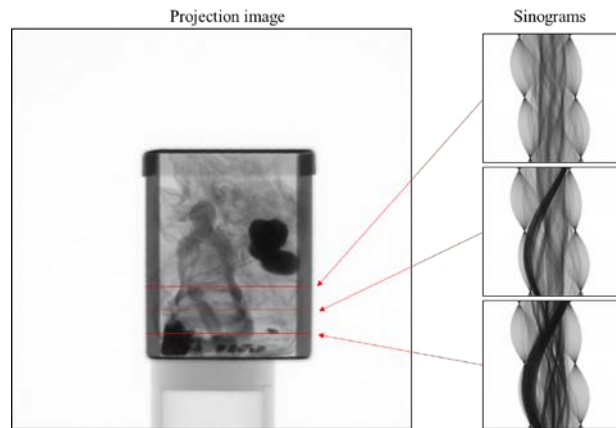


Fig. 8 Sinograms along the z-axis.

3.4 Reconstruction

After the inverse Radon transform was performed on the generated sinogram image, a cross-section image was finally obtained for the corresponding slice. Fig. 9 shows an example of a reconstructed image for one sinogram. The reversed image was taken so that the part with the object appeared white (a high pixel value). In the outermost copper box, the large Buddha body and the head of the small Buddha statue were well visible. Korean paper was also observed clearly.

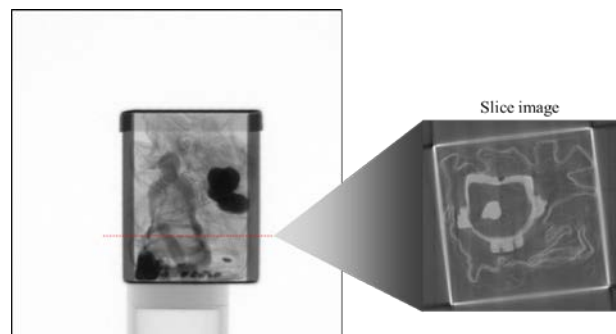


Fig. 9 Cross-sectional image for the given z-level.

When the inverse Radon transformations were performed on all sinograms, cross-sectional images of the sample can be obtained as shown in Fig. 10.

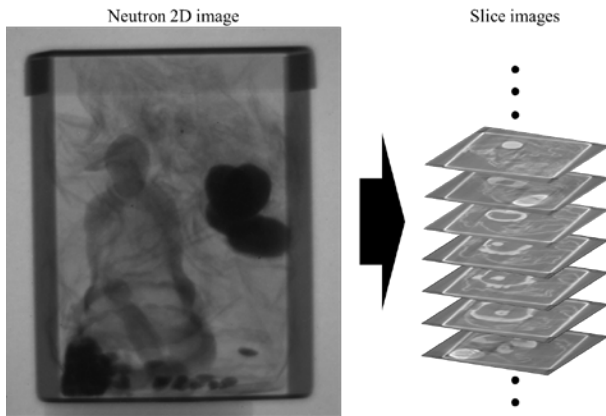


Fig. 10 A series of slice images for the various z-levels.

4. Conclusions

In the present study, we tried to develop a reconstruction code for a neutron tomography using Matlab. A series of image corrections and rotation axis corrections were performed for the reconstruction. After the sinograms were generated through rearrangement of the images, the reconstructed images were obtained using the inverse Radon transformation. As a result, the objects inside the copper box were observed without any distortion, and the components were clearly identified. We could obtain the reconstructed images by using our own code without the commercial reconstruction tool. In the future, we plan to study and apply the method to improve the image quality through various algorithms.

REFERENCES

- [1] P. Rügsegger, B. Koller, R. Müller, A microtomographic system for the nondestructive evaluation of bone architecture, *Calcif. Tissue Int.* 58 (1996) 24–29.
- [2] J.T. Dobbins III, D.J. Godfrey, Digital x-ray tomosynthesis: current state of the art and clinical potential, *Phys. Med. Biol.* 48 (2003) R65.
- [3] V. Cnudde, B. Masschaele, M. Dierick, J. Vlassenbroeck, L. Van Hoorebeke, P. Jacobs, Recent progress in X-ray CT as a geosciences tool, *Appl. Geochemistry.* 21 (2006) 826–832.